JOURNAL OF CATALYSIS **161,** 577–586 (1996)
ARTICLE NO. 0220

Structure and Electronic State of $PdCl_2$–$CuCl_2$ Catalysts Supported on Activated Carbon

Yasushi Yamamoto, Tokuo Matsuzaki, Kyoji Ohdan, and Yasuaki Okamoto*,[1]

*Ube Laboratory, Ube Industries, Ltd., 1978-5 Kogushi, Ube, Yamaguchi 755, Japan; and *Department of Chemical Engineering, Faculty of Engineering Science, Osaka University, Toyonaka, Osaka 560, Japan*

Received April 5, 1995; revised February 21, 1996; accepted March 25, 1996

The structure and electronic state of $PdCl_2$–$CuCl_2$ catalysts supported on activated carbon (AC) were characterized using XAFS techniques. On the basis of XANES of the Cu *K*-edge, a majority of $CuCl_2$ supported on the activated carbon was found to be reduced to Cu^+ species, probably by the reduction sites on the support surface. The Cu *K*-edge EXAFS and XANES results suggest that the Cu^+ species are coordinated with three Cl^- anions irrespective of the presence of $PdCl_2$. The EXAFS analysis of the Pd *K*-edge showed the formation of Pd metal particles as well as Pd chloride species coordinated with three Cl^- anions. These results are in conformity with the chemical analysis of the catalyst that indicates a considerable loss of Cl^- on the adsorption of $PdCl_2$ or $CuCl_2$ on the activated carbon. It was found that the formation of Pd metal was strongly suppressed by the presence of $CuCl_2$. The $PdCl_2$/AC, $PdCl_2$–$CuCl_2$/AC, and $CuCl_2$/AC catalysts showed CO oxidation activities at >400 K, >500 K, and >570 K, respectively. The addition of H_2O promoted the reactions over $PdCl_2$–$CuCl_2$/AC. Comparing the catalytic properties with the XAFS results, it is considered that the Pd metal particles are responsible for the low-temperature activities at >400 K. It is suggested that Cu^+ chloride species shows the activity only at >570 K.

INTRODUCTION

Palladium catalysts are used in the oxidation of organic materials, especially unsaturated aliphatic hydrocarbons, providing the corresponding aldehydes or ketones in the presence of H_2O (1, 2). In these reaction systems, Cu^{2+} compounds are necessary to reoxidize Pd^0, which is produced during the oxidation reaction, to the original Pd^{2+} species. The catalytic synergies between Pd and Cu in homogeneous reaction systems have been investigated by many workers (3–5). Homogeneous $PdCl_2$–$CuCl_2$ catalyst systems have also been reported to be active for the oxidation of CO at low temperatures (6).

For the sake of industrial convenience, heterogenized catalysts have been investigated in the Wacker process by Smidt *et al.* (2), Katz and Pismen (7), and Rao and Datta (8). The CO oxidation over supported $PdCl_2$, $CuCl_2$, and the composite catalysts was reported by Desai *et al.* (9). Recently, Choi and Vannice (10–14) have intensively studied the CO oxidation over $PdCl_2$–$CuCl_2$ catalysts supported on activated carbon and Al_2O_3 by means of IR and kinetics. It was reported that $PdCl_2$ was much more active than $CuCl_2$ and that strong synergies were generated in binary catalyst systems. Reaction intermediates were proposed to be $PdCl_2(CO)$ and $CuCl(CO)$. Carbon-supported $PdCl_2$–$CuCl_2$ catalysts showed higher activities than Al_2O_3-supported catalysts in the presence of H_2O.

Despite the fact that activated carbon (AC) is frequently used as a catalyst support to provide a high dispersion of supported metals, detailed studies on the interactions between the supported metal species and the activated carbon have rarely been reported. Shirakashi *et al.* (15) have shown that a variety of heavy metal ions or some noble metal ions are adsorbed on the activated carbon as anion complexes and in some reduced forms. The interactions between supported metal complexes and activated carbon surface, however, do not seem to be well established at present. Hence, it is of great importance to define the structure and electronic state of supported metal complexes on the activated carbon.

This work is aimed at studying the structure and electronic state of $PdCl_2$ and $CuCl_2$ supported on activated carbon by use of X-ray absorption fine structure (XAFS) techniques. We also carried out CO oxidation as a test reaction over $PdCl_2$, $CuCl_2$, and their composite catalysts supported on activated carbon and compared the catalytic behavior with the structure and electronic state of palladium and copper species on the support.

EXPERIMENTAL METHODS

Catalyst Preparation

Carbon-supported $PdCl_2$, $CuCl_2$, and $PdCl_2$–$CuCl_2$ composite catalysts were prepared by impregnating activated carbon with aqueous 5% NH_3 solutions of $PdCl_2$, $CuCl_2$,

[1] To whom correspondence should be addressed.

0021-9517/96 $18.00

and a mixture of $PdCl_2$ and $CuCl_2$, respectively. The catalyst samples were dried at 373 K for 1 h and subsequently calcined at 473 K for 2 h in a N_2 stream at atmospheric pressure. The loadings of Pd and Cu were 1.0 and 1.2 wt%, respectively, according to ICP. The chlorine content of catalyst samples was analyzed by XRF. The activated carbon employed here was Shirasagi C2X7/12 supplied by Takeda Pharmaceutical Corp. Ltd. Its surface area was about 1000 $m^2\ g^{-1}$.

XAFS Measurements

The XAFS spectra of the Pd *K*-edge and Cu *K*-edge were measured on BL-10B and BL-6B instruments of Photon Factory in the National Laboratory for High Energy Physics, respectively. The photon energies were calibrated using a Cu *K*-edge energy at 8980.3 eV for Cu metal. The catalyst samples were treated at 393 K in a N_2 stream, followed by evacuation at room temperature before the XAFS measurements. Spectra were obtained at room temperature without exposing the sample to air using an *in situ* EXAFS cell with polyimide windows. The samples which had been just dried were only evacuated at room temperature prior to XAFS measurements.

The EXAFS oscillation $\chi(k)$ was extracted from the observed data by subtracting the smoothly varying part, which was estimated by a cubic spline method, and normalizing the oscillation by the absorption of the free atom. Fourier transformation of $k^3\chi(k)$ was carried out over the region of $\Delta k = 3$–$15\ Å^{-1}$ (Cu *K*-edge) or $\Delta k = 4$–$15\ Å^{-1}$ (Pd *K*-edge). The peak in the Fourier transform was filtered and inversely transformed into k space again. The Fourier-filtered data were then analyzed by a curve-fitting technique, assuming a plane wave approximation (16). $PdCl_2$, Pd metal, $CuCl_2$, Cu metal, and CuO were used to extract experimental EXAFS parameters for Pd–Cl, Pd–Pd, Cu–Cl, Cu–Cu, and Cu–O bondings, respectively. Some of the structural parameters are summarized in Table 1.

TABLE 1

Structural Parameters as Derived from the Cu *K*-Edge and Pd *K*-Edge EXAFS

	Treatment[a]	Cl/Pd + Cu	Atom pair	C. N.	*R*/nm	E_0/eV	$\Delta\sigma^2$(Å^2)
Catalyst							
$CuCl_2$/AC	N_2	1.22	Cu–Cl	3.1	0.212	−3.9	0.0008
$PdCl_2$/AC	N_2	1.02	Pd–Cl	2.4	0.233	6.4	0.0011
			Pd–Pd	0.8	0.280	16.1	−0.0003
	$CO/O_2/H_2O$		Pd–Cl	2.6	0.232	3.5	0.0011
			Pd–Pd	1.4	0.277	11.0	−0.0007
$PdCl_2$–$CuCl_2$/AC	Dry[b]		Cu–Cl	3.2	0.211	−5.7	0.0011
	Calc.[b]		Cu–Cl	3.6	0.212	−3.9	0.0027
	N_2	1.86	Pd–Cl	2.4	0.231	1.1	0.0000
			Cu–Cl	3.1	0.211	− 6.2	0.0015
	CO[b]	1.43	Cu–Cl	2.5	0.214	−1.1	−0.0001
	CO/O_2	1.25	Pd–Cl	2.8	0.231	1.9	0.0003
			Cu–Cl	2.8	0.213	− 2.6	0.0005
	$CO/O_2/H_2O$[c]		Pd–Cl	2.9	0.232	1.1	0.0004
Reference compounds							
$PdCl_2$[d]	Dehydrated		Pd–Cl	4.0	0.231		
$CuCl_2$[e]	Dehydrated		Cu–Cl	4.0	0.230		
$CuCl_2 \cdot H_2O$[f]			Cu–Cl	2.0	0.231		
			Cu–Cl	2.0	0.298		
			Cu–O	2.0	0.201		
Pd metal[f]			Pd–Pd	12	0.275		

[a] N_2, treated at 393 K in a N_2 stream at atmospheric pressure after calcination; dry, dried at 393 K after impregnation; calc., after calcination in a N_2 stream at 473 K; CO, treated at 393 K in flowing CO at 1 atm; CO/O_2, after CO oxidation at 473 K for 1 h; $CO/O_2/H_2O$, after CO oxidation in the presence of H_2O.

[b] Pd *K*-edge EXAFS was not measured.

[c] Cu *K*-edge EXAFS was not measured.

[d] Ref. (25).

[e] Ref. (26).

[f] Ref. (27).

CO Oxidation Reaction

The CO oxidation reaction was carried out using a fixed-bed flow reactor (6 mm in diameter) made of quartz at atmospheric pressure. The reaction gas mixture (composition: CO, 0.2%, O_2, 2%; He, balance) was passed through the catalyst (0.05 g) at a space velocity of 10,000 h^{-1}. The flow rate (20 cm^3 min^{-1}, STP) was controlled using calibrated mass flow controllers (Ueshima-Brooks, 5850E). The catalyst was placed in the reactor and pretreated in He at 473 K for 1 h and then cooled to 300 K, followed by the CO oxidation reaction. The catalyst was stayed at room temperature for 0.5–1 h in the stream of the reaction gas before starting the reaction. The reaction temperature was increased from room temperature to 600 K at a rate of 6 K min^{-1}. The CO consumption and CO_2 formation were analyzed by means of an on-line GC with columns of Molecular Sieve 5A and Porapac Q, respectively. The effects of H_2O addition on the CO oxidation over the Pd and Cu chloride catalysts were examined. The water vapor pressure was controlled by bubbling the feed gas through a water reservoir immersed in an ice bath. The pressure of water was not determined.

RESULTS AND DISCUSSION

Structure and Electronic State of Catalysts

The XANES spectra of the Cu *K*-edge for supported copper catalysts have been used to obtain information about the electronic state of copper species (17–19). The normalized Cu *K*-edge XANES spectra for the catalysts are compared in Fig. 1 with that of unsupported, dehydrated $CuCl_2$ as a reference. A weak preedge peak at 8979 eV for $CuCl_2$ is ascribed to an electron transition of the 1*s* level to the vacant 3*d* level, being characteristic of the Cu^{2+} electronic state (20). The $1s \rightarrow 3d$ preedge peak was not observed for the supported $CuCl_2$ catalyst as shown in Fig. 1a. The $1s \rightarrow 3d$ transition is dipole forbidden and thereby the intensity strongly depends both on the local symmetry and the valence state of the atoms concerned. In the case of $CuCl_2$, Cu^{2+} is in a distorted square-planar symmetry, resulting in a relatively strong $1s \rightarrow 3d$ transition peak. The disappearance of the preedge peak for $CuCl_2$/AC might be explained assuming a higher symmetry of Cu^{2+} species or the formation of Cu^+ species ($3d^{10}$) by the reduction of Cu^{2+}. However, a symmetry such as an octahedra for Cu^{2+} chloride species is unusual and the EXAFS analysis suggests only $3Cl^-$ around Cu atoms (*vide infra*). Consequently, the fact that the preedge peak due to the $1s \rightarrow 3d$ transitions disappear for $CuCl_2$/AC indicates the formation of Cu^+ species in conformity with a great increase in the peak intensity of a $1s \rightarrow 4p\pi^*$ transition as discussed below.

The XANES structure of the $CuCl_2$/AC catalyst is significantly different from that of $CuCl_2$. Dehydrated $CuCl_2$ (Fig. 1g) exhibited a XANES structure characteristic of Cu^{2+} species. The XANES of $CuCl_2$ is composed of two sets of doublet peaks. They are assigned to $1s \rightarrow 4p\pi^*$ (8984 and 8989 eV) and $1s \rightarrow 4p\sigma^*$ (8989 and 8994 eV) transitions (21–24). Final state effects (core-hole screening) on the electronic transition of Cu^{2+} species are proposed to cause the doublet peaks corresponding to well-screened and poorly screened core-hole states, as usually observed with the satellite structures of Cu2*p* XPS spectra for the Cu^{2+} species. On the other hand, $CuCl_2$ supported on AC (Fig. 1a) showed only two peaks: a sharp peak at 8984 eV and a broad peak at 8997 eV, being assignable to single

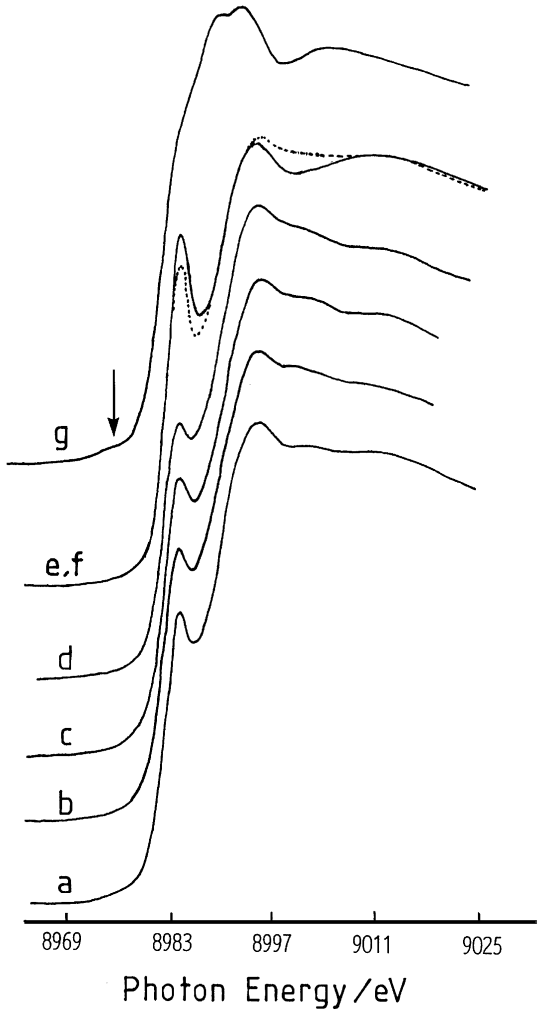

FIG. 1. Normalized Cu *K*-edge XANES spectra for $PdCl_2$–$CuCl_2$ catalysts (a) $CuCl_2$/AC treated at 393 K for 1 h in a N_2 stream at atmospheric pressure after calcination; (b) $PdCl_2$–$CuCl_2$/AC after drying at 373 K, following impregnation; (c) $PdCl_2$–$CuCl_2$/AC after calcination in N_2 at 473 K; (d) $PdCl_2$–$CuCl_2$/AC treated at 393 K in a N_2 stream after calcination; (e) $PdCl_2$–$CuCl_2$/AC after a CO treatment at 393 K for 1 h (solid line); (f) $PdCl_2$–$CuCl_2$/AC after CO oxidation at 473 K for 1 h (dotted line); and (g) $CuCl_2$ dehydrated *in vacuo* at 473 K. An arrow shows a preedge peak.

bands of $1s \rightarrow 4p\pi^*$ and $1s \rightarrow 4p\sigma^*$ transitions, respectively (21–24). These spectral features are characteristic to Cu^+ ($3d^{10}$) species as observed for various Cu^+ compounds (20).

The Cu *K*-edge XANES spectra for $PdCl_2$–$CuCl_2$/AC in Fig. 1b–1d also indicate the formation of Cu^+ species; the disappearance of the preedge peak and the appearance of a strong single peak $1s \rightarrow 4p\pi^*$ transition. It is evident that the Cu^+ species is formed even in the sample that has been just dried at 373 K after impregnation (Fig. 1b). Calcination at 473 K in a N_2 stream did not change any spectral features (Fig. 1c). The Cu-XANES spectrum of $PdCl_2$–$CuCl_2$/AC did not vary with a further treatment at 393 K in a stream of N_2 (Fig. 1d).

Representative EXAFS functions $\chi(k)$ multiplied by k^3 and the corresponding Fourier transforms of the Cu *K*-edge EXAFS are shown for $PdCl_2$–$CuCl_2$/AC in Figs. 2 and 3, respectively. The structural data derived from EXAFS analysis are summarized in Table 1 as well as those of relevant reference compounds. The curve-fitting results are presented in Fig. 4 ($\Delta R = 0.11$–0.21 nm). The EXAFS oscillations were found to be reasonably well curve fitted assuming only Cu–Cl bondings. The contributions of Cu–O

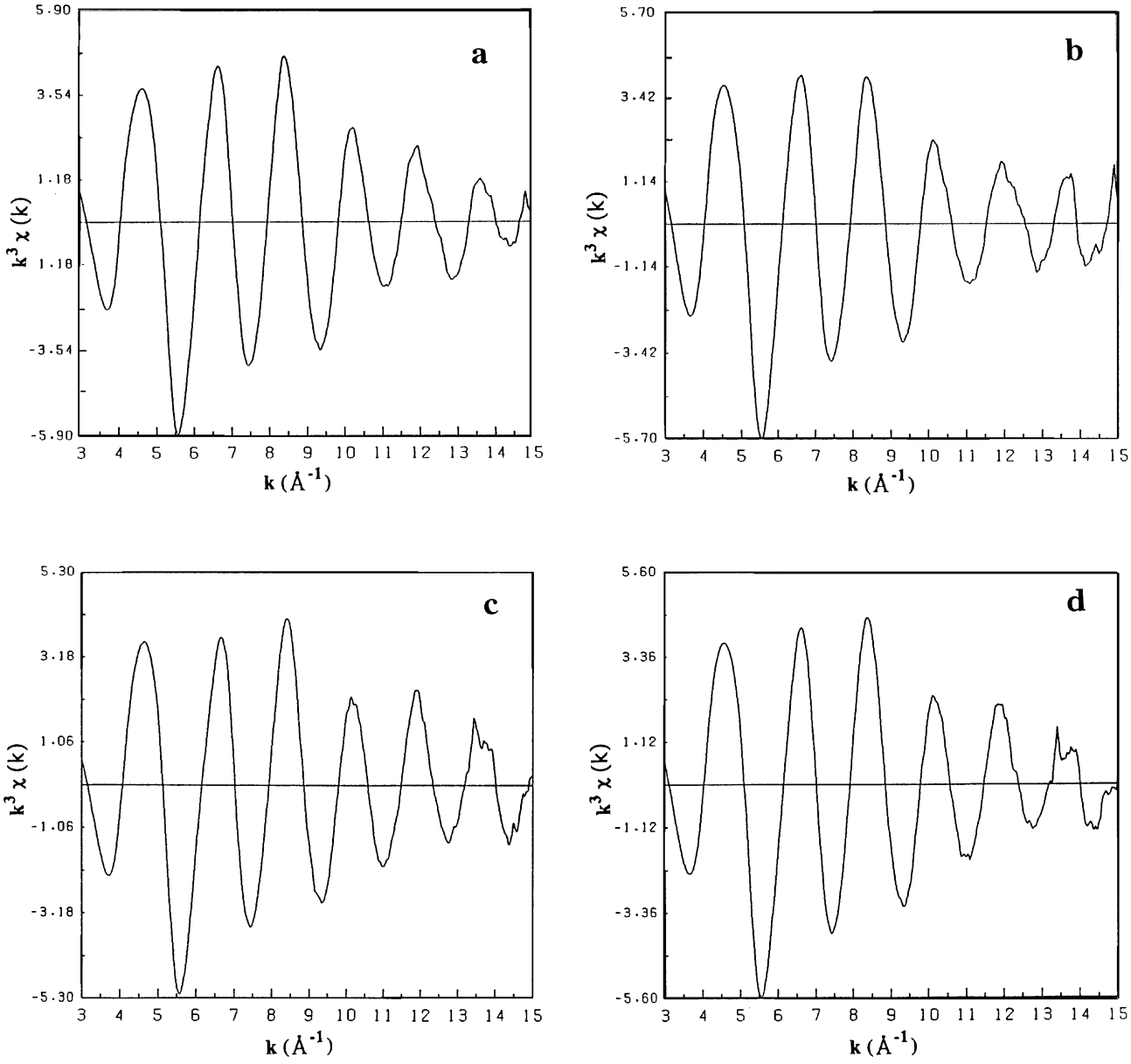

FIG. 2. k^3-weighted EXAFS oscillations of Cu *K*-edge for (a) $CuCl_2$/AC treated in N_2 at 393 K after calcination; (b) $PdCl_2$–$CuCl_2$/AC treated in N_2 at 393 K after calcination; (c) $PdCl_2$–$CuCl_2$/AC treated in a stream of CO at 393 K for 1 h; and (d) $PdCl_2$–$CuCl_2$/AC after CO oxidation at 473 K for 1 h.

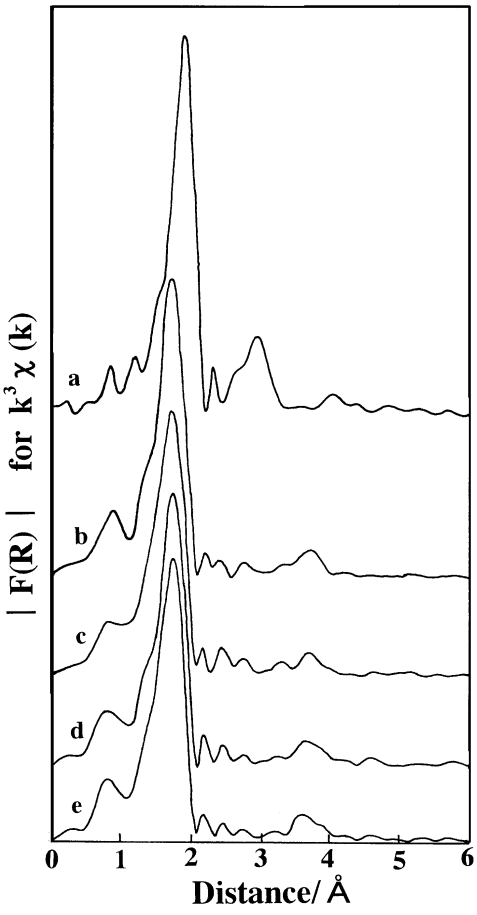

FIG. 3. Fourier transforms of k^3-weighted Cu *K*-edge EXAFS for $PdCl_2$–$CuCl_2$/AC catalysts ($\Delta k = 3$–15 Å^{-1}). (a) $CuCl_2$ dehydrated; (b) $CuCl_2$/AC treated in N_2 at 393 K after calcination; (c) $PdCl_2$–$CuCl_2$/AC treated in a stream of N_2 at 393 K after calcination; (d) $PdCl_2$–$CuCl_2$/AC treated in a stream of CO at 393 K for 1 h; and (e) $PdCl_2$–$CuCl_2$/AC after CO oxidation at 473 K for 1 h.

and Cu–C bondings are, if any, considered to be comparatively small.

With $CuCl_2$/AC treated in a N_2 stream at 393 K, the distance of the Cu–Cl bond is calculated to be 0.211 nm, which is significantly shorter than that of bulk $CuCl_2$ (0.230 nm) (26) or $CuCl_2 \cdot H_2O$ (0.231 nm) (27). The Cu–Cl bond length for $CuCl_2$/AC is rather close to that reported for a cuprous chloride, Cu_3Cl_3 (0.216 nm) (28), suggesting the formation of Cu^+ chloride species upon the impregnation of $CuCl_2$ on AC. This is quite consistent with the XANES results. The coordination number of Cu is estimated to be about three. As shown in Table 1, the chlorine content was found to be Cl/Cu = 1.22 and significantly smaller than the original value of Cl/Cu = 2, indicating that the adsorption of $CuCl_2$ on AC is accompanied by a partial loss of Cl^- anions. The Cu–Cl bond distance and coordination numbers for $PdCl_2$–$CuCl_2$/AC catalysts are very close to those of $CuCl_2$/AC, after the drying, calcination or N_2 treatment.

According to Kau *et al.* (20), the relative intensity of the peak due to a $1s \rightarrow 4p\pi^*$ transition at 8984 eV in the Cu *K*-edge XANES varies with the coordination number of Cu^+ species. Comparing with the Cu XANES reported by them, the coordination number of the Cu^+ species formed on AC is estimated to be about three (Fig. 1a–1d). This is in excellent agreement with the structural parameters derived from the EXAFS results.

On the basis of the Cu–Cl bond distance, coordination number and Cu *K*-edge XANES features, it is concluded that the structure and electronic state of copper species supported on AC is completely different from those of $CuCl_2$ and that a majority of copper species is reduced to Cu^+ coordinated with three Cl^- anions. It is also suggested that the addition of $PdCl_2$ does not affect the formation and local structure of the Cu^+ chloride species.

The $1s \rightarrow 4p\pi^*$ peak at 8984 eV for $PdCl_2$–$CuCl_2$/AC (Fig. 1e) was apparently intensified by treating the sample at 393 K with CO at atmospheric pressure, suggesting a further increase in the proportion of Cu^+ species and/or a change in the local structure of the Cu^+ species. In the latter case, a decrease in the coordination number of Cu^+ species is suggested by the XANES study by Kau *et al.* (20). Both cases are possible and are corroborated by further decreases in the Cu–Cl coordination number and in the content of Cl^- anions upon the CO treatment as summarized in Table 1. The XANES structure of Cu *K*-edge for $PdCl_2$–$CuCl_2$/AC was varied by the CO oxidation at 473 K as compared in Fig. 1f. It is evident that the peak intensity at 8984 eV is significantly stronger than that for the calcined catalyst (Fig. 1c) but weaker than that of the CO treated catalyst (Fig. 1e), indicating that a part of the Cu^+ species is oxidized during the CO oxidation. It is conceivable that the Cu^{2+}/Cu^+ ratio is equilibrated at 473 K with the O_2/CO pressure ratio.

The background subtracted EXAFS functions $\chi(k)$ multiplied by k^3 and corresponding Fourier transforms of Pd *K*-edge EXAFS are depicted in Figs. 5 and 6, respectively. The results of the curve fittings are shown in Fig. 7 and the EXAFS parameters thus obtained are summarized in Table 1. As for the fresh $PdCl_2$/AC, Pd–Pd bondings are found at ca. 0.26 nm in Fig. 6a (phase shifts: uncorrected) as well as Pd–Cl bondings. The Pd–Pd bond distance (0.28 nm) of the $PdCl_2$/AC is close to that of Pd metal, suggesting a partial reduction of $PdCl_2$ to Pd metal particles by a mere impregnation of $PdCl_2$ onto AC. In the presence of $CuCl_2$, on the other hand, no Pd–Pd bonding was observed. It is evident that the reduction of $PdCl_2$ is strongly suppressed by the presence of $CuCl_2$. It is estimated from Table 1 that the Pd^{2+} cations in the $PdCl_2$–$CuCl_2$/AC catalyst are coordinated by three Cl^- anions as the Cu^+ species are, in conformity with a considerable loss of Cl^- anions upon the impregnation of $PdCl_2$ (Table 1).

After the CO oxidation reaction at 473 K for 1 h, no Pd metal formation was observed for $PdCl_2$–$CuCl_2$/AC by

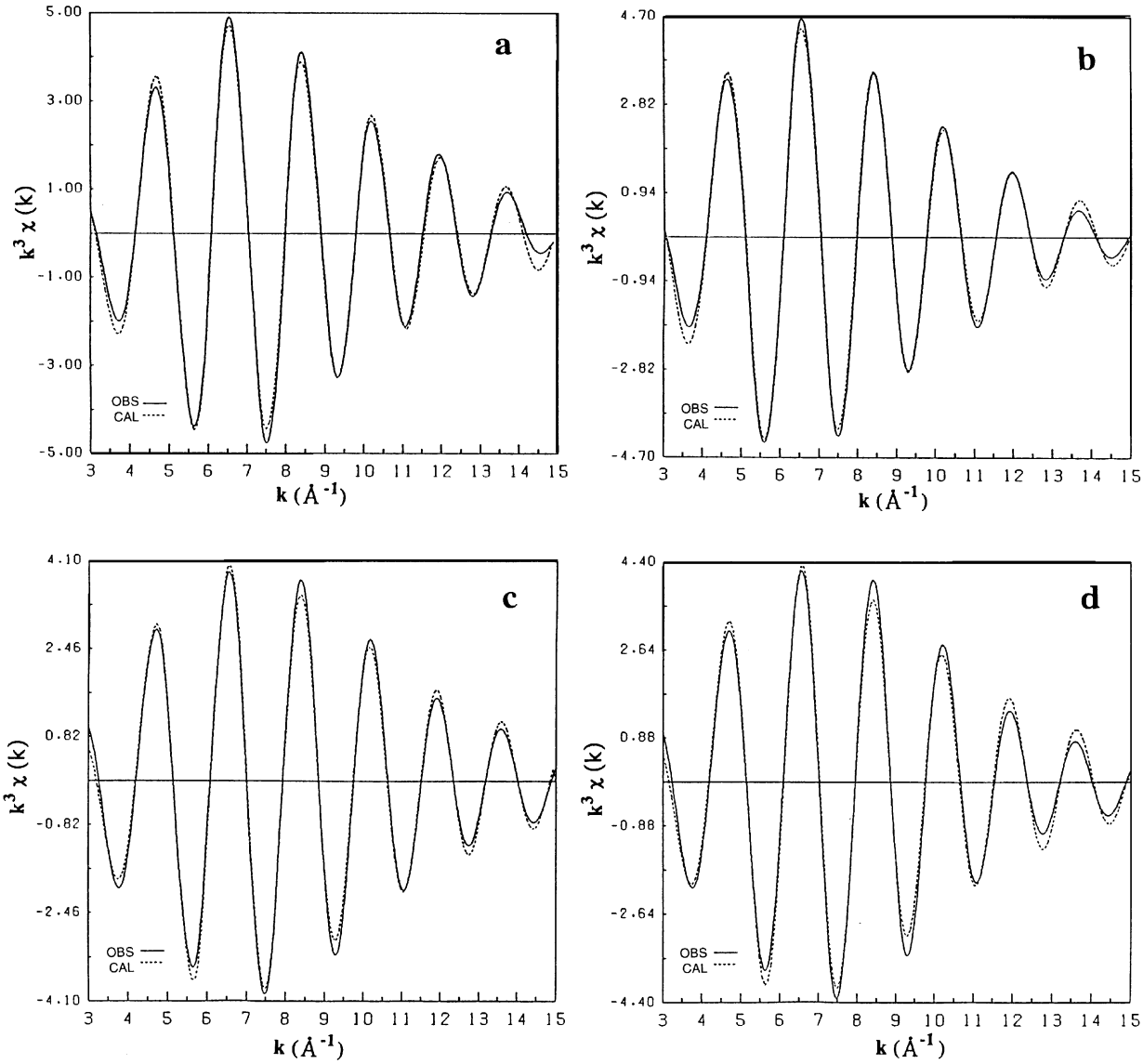

FIG. 4. k^3-weighted Fourier-filtered EXAFS functions of the Cu *K*-edge for $PdCl_2$–$CuCl_2$/AC catalysts ($\Delta R = 0.11$–0.21 nm). Solid line, observed; and dotted line, calculated. (a) $CuCl_2$/AC treated in N_2 after calcination; (b) $PdCl_2$–$CuCl_2$/AC treated in N_2 at 393 K after calcination; (c) $PdCl_2$–$CuCl_2$/AC treated in a stream of CO at 393 K for 1 h; and (d) $PdCl_2$–$CuCl_2$/AC after CO oxidation at 473 K for 1 h.

EXAFS as shown in Fig. 6c and Table 1. The formation of Pd metal on $PdCl_2$/AC was found to be promoted by CO oxidation reaction in the presence of H_2O (Fig. 6d). However, the presence of $CuCl_2$ evidently suppressed the formation of Pd metal under the same conditions (Fig. 6e).

In the present study on $PdCl_2$–$CuCl_2$/AC catalysts, Cu–Cu, Pd–Pd, or Cu–Pd bondings are not explicitly detected by the Cu and Pd *K*-edge EXAFS analyses, indicating that Cu and Pd chlorides are well dispersed over the AC surface.

It is considered that the Cu^+ chloride species and Pd^0 species are generated on reduction sites of AC. It is well established that oxygen-containing functional groups, such as carboxylic, carbonyl, and quinonyl groups, are present on the surface of activated carbon (28). The reduction of Fe^{3+} to Fe^{2+} was used to identify the quinonyl group on AC (29, 30). These functional groups are considered to work as the reduction sites of AC as exemplified in Fig. 8. A possible mechanism of the loss of Cl^- anions on the impregnations of $CuCl_2$ and $PdCl_2$ on AC is also proposed in Fig. 8.

The findings that the addition of $CuCl_2$ in $PdCl_2$/AC catalyst prevents the reduction of Pd^{2+} to Pd metal may be explained in terms of a preferential reduction of Cu^{2+} to that of Pd^{2+} on the reduction sites because of a lower redox potential of Cu^{2+} to Cu^+ (0.15 V vs. Ag^+/AgCl) than that of Pd^{2+} to Pd^0 (0.92 V) (31). Alternatively, direct

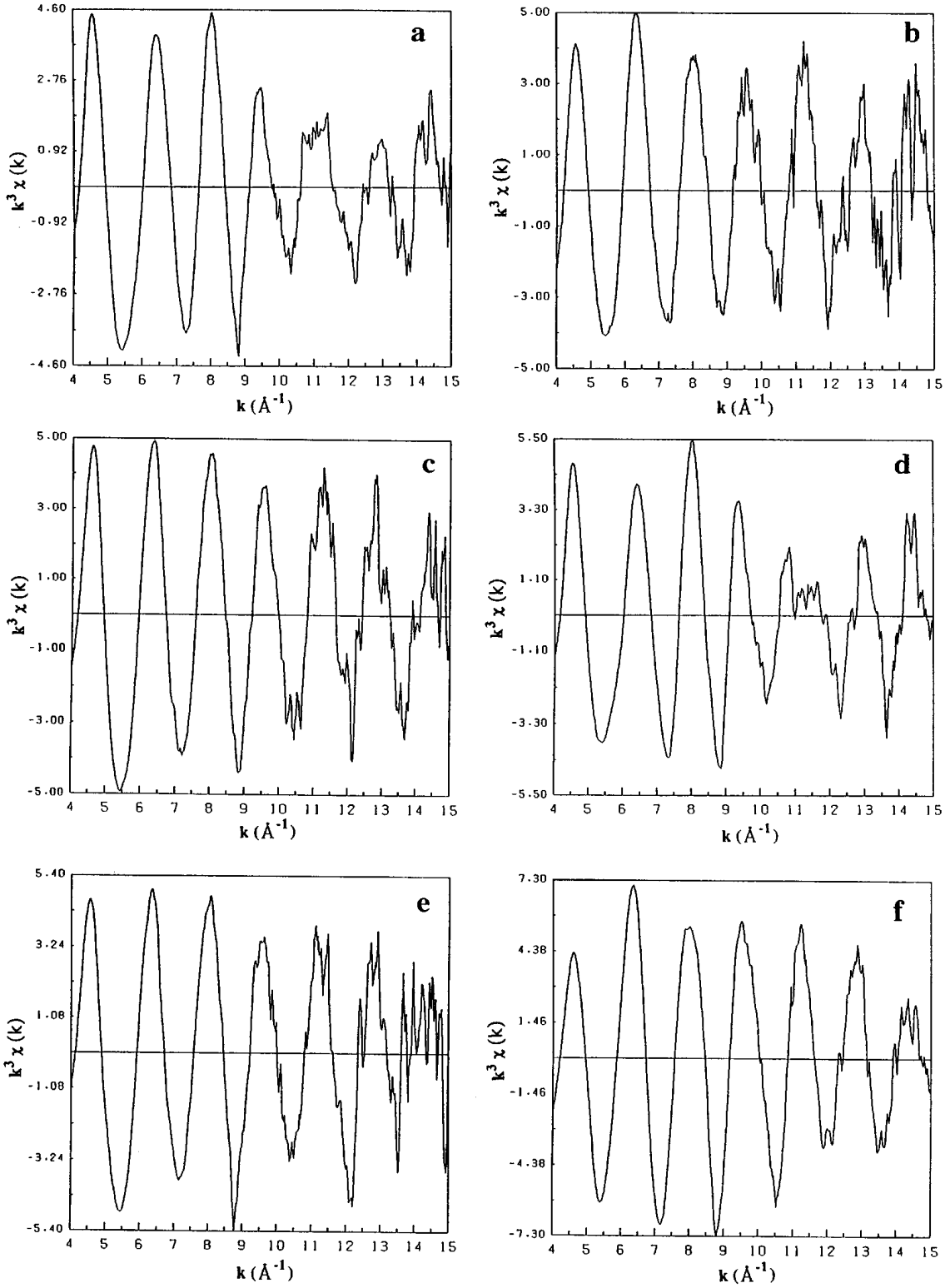

FIG. 5. k^3-weighted EXAFS oscillations of the Pd *K*-edge for (a) $PdCl_2$/AC and (b) $PdCl_2$–$CuCl_2$/AC treated in N_2 at 383 K after calcination; (c) $PdCl_2$–$CuCl_2$/AC after CO oxidation at 473 K for 1 h; (d) $PdCl_2$/AC after CO oxidation at 473 K for 1 h in the presence of H_2O; (e) $PdCl_2$–$CuCl_2$/AC after CO oxidation in the presence of H_2O; and (f) $PdCl_2$ reference compound.

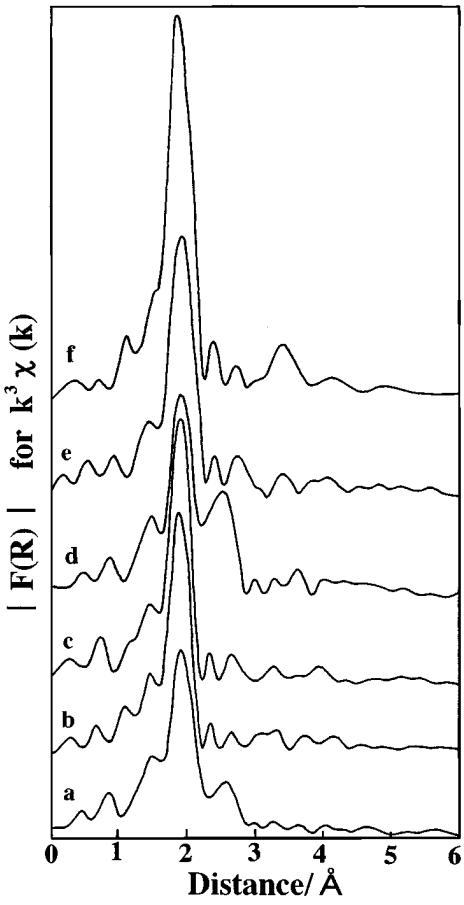

FIG. 6. Fourier transforms of k^3-weighted Pd *K*-edge EXAFS ($\Delta k = 4$–15 Å^{-1}) for $PdCl_2$–$CuCl_2$/AC catalysts. (a) $PdCl_2$/AC and (b) $PdCl_2$–$CuCl_2$/AC treated in N_2 after calcination; (c) $PdCl_2$–$CuCl_2$/AC after CO oxidation at 473 K for 1 h; (d) $PdCl_2$/AC after CO oxidation at 473 K for 1 h in the presence of H_2O; (e) $PdCl_2$–$CuCl_2$/AC after CO oxidation at 473 K for 1 h in the presence of H_2O; and (f) $PdCl_2$ reference compound.

Cu–Cl–Pd interactions or interactions between $CuCl_2$ and $PdCl_2$, through electroconductive AC surfaces may induce the oxidation of Pd^0 to Pd^{2+}, accompanied by the reduction of Cu^{2+} to Cu^+. The latter process is generally claimed to occur during the catalytic oxidation of olefins using $PdCl_2$–$CuCl_2$ Wacker-type catalysts in homogeneous systems.

It is demonstrated above that the extent of reduction of Pd^{2+} in $PdCl_2$/AC is considerably increased, relative to that of the fresh $PdCl_2$/AC, during the CO oxidation in the presence of H_2O, whereas the reduction of Pd^{2+} is significantly suppressed in $PdCl_2$–$CuCl_2$/AC. In addition, a part of Cu^+ species in $PdCl_2$–$CuCl_2$/AC is oxidized during the oxidation reaction as shown in Fig. 1f. Consequently, it is surmised that with $PdCl_2$–$CuCl_2$/AC there is a process in which Pd^0 species is oxidized by the Cu^{2+} species, forming Pd^{2+} and Cu^+ species. At present, we cannot conclude from the EXAFS results whether there are direct bondings between Cu and Pd chloride phases.

CO Oxidation Reaction

We examined the relation between the structure and electronic state of $PdCl_2$–$CuCl_2$ catalysts and the catalytic CO oxidation as a test reaction. The results on CO oxidation are shown in Fig. 9. The $PdCl_2$/AC catalyst showed a significant CO oxidation activity at above 470 K and about 100% of CO conversion was attained at >550 K. The addition of H_2O to the reaction system promoted the activity of $PdCl_2$/AC. The EXAFS results in Table 1 indicate the increase of Pd metal formation. Besides, the activity of $PdCl_2$–$CuCl_2$/AC was much lower than that of $PdCl_2$/AC. As demonstrated above, the formation of Pd metal is strongly suppressed in the presence of $CuCl_2$. Accordingly, the active species are considered to be Pd metal particles formed by reduction of $PdCl_2$ by AC or during the reaction. The findings that Pd/zeolite, in which Pd^{2+} is easily reduced to Pd metal, showed very high activity for the CO oxidation at 400–430 K under the same reaction conditions, provide further evidence to the above conclusion (32). Adsorbed water on the activated carbon is considered to accelerate the formation of Pd^0 by the following reactions. $PdCOCl_2$ species is not so stable in the presence of hydroxyl groups.

$$PdCl_2 + CO \rightarrow PdCOCl_2$$

$$PdCOCl_2 + H_2O_{ads} \rightarrow Pd^0 + CO_2 + 2HCl.$$

Manchot and Konig first reported a compound with a formula, $PdCOCl_2$ (33), and the structure of $[Pd_2(CO)_2Cl_4]$ was proposed by Calderazzo and Dell'Amico (34). Choi and Vannice (10–14) have proposed that $PdCOCl_2$ is the active species in the CO oxidation over $PdCl_2$/AC.

The $CuCl_2$/AC catalyst showed two activity regions at about 370–420 K and at above 570 K. However, the total amount of CO_2 formed in the low-temperature region was calculated to be $\frac{1}{4}$–$\frac{1}{10}$ of the Cu content in the catalyst used (1.2 wt% Cu, 0.05 g catalyst) in the reaction, suggesting that the CO_2 formation at ca. 400 K is not a catalytic process but a stoichiometric chemical process such as the reduction of Cu^{2+} species to Cu^+ species. In the presence of H_2O, the low-temperature peak disappeared with $PdCl_2$–$CuCl_2$/AC. This is possibly the result of promoted reduction of Cu^{2+} species by H_2O, as shown above for $PdCl_2$, during the contact of the catalyst at room temperature with the reaction gas before ramping the reaction temperature.

The Cu^+ species may be the active species at above 570 K.

$$CuCl + CO \rightarrow CuCl(CO)_{ads}$$

$$CuCl(CO)_{ads} + 1/2O_2 \rightarrow CuCl + CO_2.$$

Similar mechanisms for CO oxidation by Cu species have been proposed by Choi and Vannice (10–14). However, it is also possible that Cu^0 particles or CuO particles formed

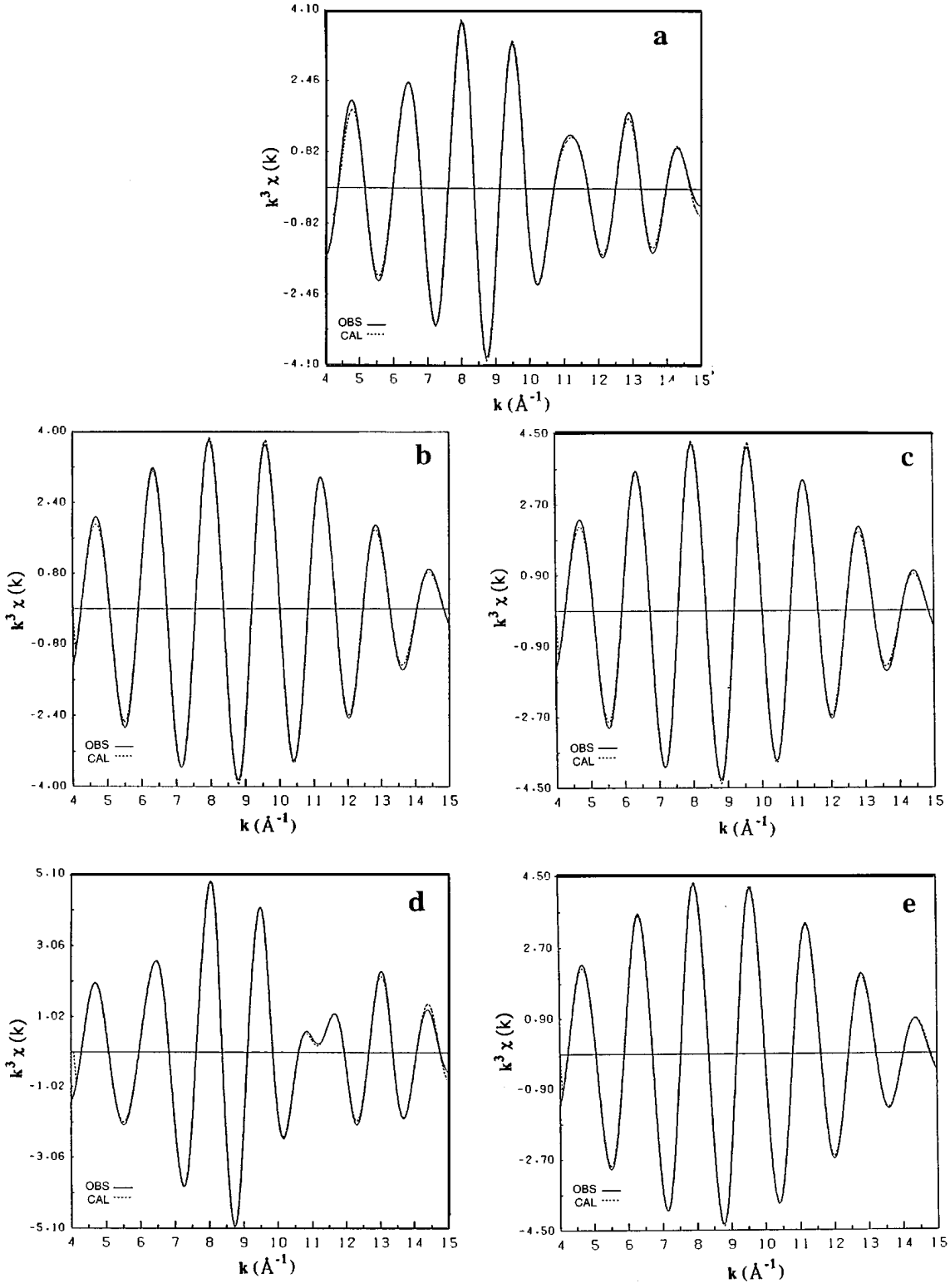

FIG. 7. k^3-weighted Fourier-filtered EXAFS functions of the Pd *K*-edge for $PdCl_2$/AC ($\Delta R = 0.1$–0.29 nm) and $PdCl_2$–$CuCl_2$/AC catalysts ($R = 0.1$–0.23 nm). Solid line, observed; and dotted line, calculated. (a) $PdCl_2$/AC treated in N_2 after calcination; (b) $PdCl_2$–$CuCl_2$/AC treated in N_2 after calcination; (c) $PdCl_2$–$CuCl_2$/AC after CO oxidation at 473 K for 1 h; (d) $PdCl_2$/AC after CO oxidation at 473 K for 1 h in the presence of H_2O; and (e) $PdCl_2$–$CuCl_2$/AC after CO oxidation at 473 K for 1 h in the presence of H_2O.

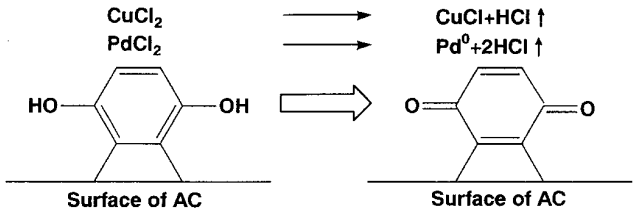

FIG. 8. Schematic reduction mechanism of Cu^{2+} or Pd^{2+} chloride species supported on AC.

by the decomposition of Cu^{+} chloride species are active for the reaction at >570 K.

CONCLUSIONS

The structure and electronic state of $PdCl_2$–$CuCl_2$ composite catalysts supported on activated carbon were investigated using XAFS techniques. On the basis of the XANES of the Cu *K*-edge, it is concluded that a majority of $CuCl_2$ is reduced to Cu^{+} species by the reduction sites of the activated carbon during the catalyst preparation. The Cu *K*-edge EXAFS and XANES results manifest that the Cu^{+} species is coordinated with three Cl^{-} anions. The EXAFS analysis of the Pd *K*-edge suggests that the Pd^{2+} species on AC are also coordinated with three Cl^{-} anions, accompanied by a partial reduction of Pd^{2+} to Pd metal aggregates. These results are consistent with a loss of Cl^{-} on the impregnation of $PdCl_2$ or $CuCl_2$ onto the activated carbon. It is revealed that the formation of Pd metal is strongly suppressed in the presence of $CuCl_2$.

The $PdCl_2$–$CuCl_2$/AC catalysts showed the CO oxidation activities at 370–420 K and above 500 K. The addition of H_2O increased the activity of $PdCl_2$–$CuCl_2$/AC. In comparison with the XAFS results, it is considered that the Pd^{0} particles are responsible for the reaction at >400 K. The Cu^{+} species are suggested to show the activity for CO oxidation reaction at >570 K.

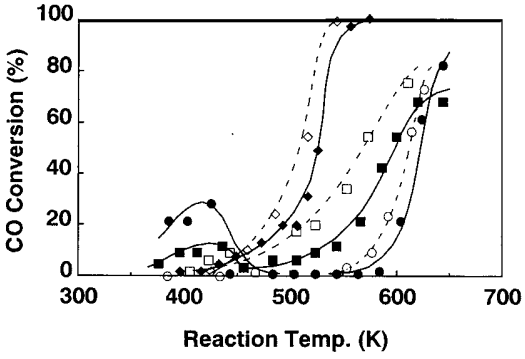

FIG. 9. Activity of $PdCl_2$–$CuCl_2$/AC catalyst for CO oxidation. (●) $CuCl_2$/AC, (◆) $PdCl_2$/AC, and (■) $PdCl_2$–$CuCl_2$/AC (solid line) in the absence of H_2O; and (○) $CuCl_2$/AC, (◇) $PdCl_2$/AC, and (□) $PdCl_2$–$CuCl_2$/AC (dotted line) in the presence of H_2O.

ACKNOWLEDGMENTS

We are grateful to Professors H. Kuroda and N. Kosugi for providing us the EXAFS analysis program (EXAFS 1). We also express our sincere thanks to Professor M. Nomura, Dr. N. Usami, and the staff of the Photon Factory, National Laboratory for High Energy Physics, for assistance in measuring XAFS spectra (Proposal 91-183).

REFERENCES

1. Maitlis, P. M., "The Organic Chemistry of Palladium," Vols. 1 and 2. Academic Press, New York, 1971; Tsuji, J., *Synthesis* 369 (1984).
2. Smidt, J., Hafner, W., Jira, R., Sedlmeier, J., Ruttinger, R., and Kojer, H., *Angew. Chem.* **71**, 176 (1959).
3. McQullin, F. J., and Parker, D. G., *J. Chem. Soc. Perkin I* 809 (1974).
4. Henry, P. M., "Palladium Catalyzed Oxidation of Hydrocarbons," Reidel, Dordrecht, 1980.
5. Tsuji, J., Shimizu, I., and Yamamoto, K., *Tetrahedron Lett.* 2975 (1976).
6. Lloyd, W. G., and Rowe, D. R., Canadian Patents 3790662, 1974, and 1011531, 1977.
7. Katz, G., and Pismen, L. M., *Chem. Eng. J.* **18**, 203 (1979).
8. Rao, V., and Datta, R., *J. Catal.* **114**, 377 (1988).
9. Desai, M. N., Butt, J. B., and Dranoff, J. S., *J. Catal.* **79**, 95 (1983).
10. Choi, K. I., and Vannice, M. A., *J. Catal.* **127**, 465 (1991).
11. Choi, K. I., and Vannice, M. A., *J. Catal.* **127**, 489 (1991).
12. Choi, K. I., and Vannice, M. A., *J. Catal.* **131**, 1 (1991).
13. Choi, K. I., and Vannice, M. A., *J. Catal.* **131**, 22 (1991).
14. Choi, K. I., and Vannice, M. A., *J. Catal.* **131**, 36 (1991).
15. Shirakashi, T., Tsuruta, K., Kajii, K., and Kuriyama, M., *Nippon Kagakukai-shi* 1330 (1984).
16. Kosugi, N., and Kuroda, H., Program EXAFS 1/VO4, Research Center for Spectrochemistry, Faculty of Science, University of Tokyo, Tokyo, 1987.
17. Clausen, B. S., Lengeler, B., and Rasmussen, B. S., *J. Phys. Chem.* **89**, 2319 (1985).
18. Tohji, K., Udagawa, Y., Mizushima, T., and Ueno, A., *J. Phys. Chem.* **89**, 5671 (1985).
19. Tzou, M. S., Kusunoki, M., Asakura, K., Kuroda, H., Moretti, G., and Sachtler, W. M. H., *J. Phys. Chem.* **95**, 5210 (1991).
20. Kau, L. S., Spira-Solomon, D. J., Penner-Hahn, J. E., Hodgson, K. O., and Solomon, E. I., *J. Am. Chem. Soc.* **109**, 6433 (1987).
21. Kosugi, N., Yokoyama, T., Asakura, K., and Kuroda, H., *Chem. Phys.* **91**, 249 (1984).
22. Yokoyama, T., Kosugi, N., and Kuroda, H., *Chem. Phys.* **103**, 101 (1986).
23. Kosugi, N., Tokura, Y., Takagi, H., and Uchida, S., *Phys. Rev.* **B41**, 131 (1991).
24. Bianconi, A., Li, C., Campanell, F., Della Longa, S., Pettini, I., Pampa, M., Turu, S., and Udron, D., *Phys. Rev.* **B44**, 4560 (1991).
25. Kiriyama, R., and Kiriyama, H., *in* "Kozo Muki Kagaku (Structural Inorganic Chemistry)," p. 109. Kyoritsu, Tokyo, 1964. [In Japanese]
26. Cotton, F. A., and Wilkinson, G., *in* "Advanced Inorganic Chemistry," 5th ed., p. 766. Wiley, New York, 1988.
27. Cotton, F. A., and Wilkinson, G., *in* "Advanced Inorganic Chemistry," 5th ed., p. 759. Wiley, New York, 1988.
28. Boehm, H. P., and Knözinger, H., "Catalysis" (J. R. Anderson and M. Boudart Eds.), Vol. 4, p. 39. Springer-Verlag, New York, 1983.
29. Boehm, H. P., *Adv. Catal.* **16**, 179 (1966).
30. Donnet, J. B., *Carbon* **6**, 161 (1968).
31. Izatt, R. M., Eatough, D., and Christensen, J. J., *J. Chem. Soc.* 1301, (1967).
32. Yamamoto, Y., Okamoto, Y., *et al.,* unpublished results.
33. Manchot, W., and Konig, J., *J. Chem. Ber.* **59**, 883 (1926).
34. Calderazzo, F., and Dell'Amico, D. B., *Inorg. Chem.* **20**, 1310 (1981).